HHS Public Access

Author manuscript

ACS Chem Biol. Author manuscript; available in PMC 2019 December 05.

Published in final edited form as:

ACS Chem Biol. 2018 November 16; 13(11): 3059–3064. doi:10.1021/acschembio.8b00767.

Selective usage of isozymes for stress response

Yugang Zhang, **Zhewang Lin**, **Miao Wang**, **Hening Lin**

Howard Hughes Medical Institute, Department of Chemistry and Chemical Biology, Cornell University, Ithaca, NY 14853, USA

Abstract

Isozymes are enzymes with similar sequences that catalyze the same reaction in a given species. In *Saccharomyces cerevisiae*, most isozymes have major isoforms with high expression levels and minor isoforms with little expression in normal growth conditions. In a proteomic study aimed to identify yeast protein regulated by rapamycin, we found an interesting phenomenon that for several metabolic enzymes, the major isozymes are downregulated while the minor isozymes are upregulated. Through enzymological and biochemical studies, we demonstrate that a rapamycin-upregulated enolase isozyme (ENO1) favors gluconeogenesis and a rapamycin-upregulated alcohol dehydrogenase isozyme (ALD4) promotes the reduction of NAD^+ to NADH (instead of $NADP^+$ to NADPH). Gene deletion study in yeast showed that the ENO1 and ALD4 are important for yeast survival in less favorable growth conditions. Our study thus highlights the different metabolic needs of cells under different conditions and how nature chooses different isozymes to fit the metabolic needs.

Metabolic enzymes that catalyze cellular biochemical transformations are essential for all living organisms. In any given species, there typically exist multiple enzymes that catalyze the same biochemical reaction and thus are called isozymes(1). For example, humans have three isocitrate dehydrogenases that catalyze the conversion of isocitrate to α-ketoglutarate, a step in the citric acid cycle(2). Isozymes allows differential regulation, such as tissue expression pattern, subcellular localization, and post-translational modifications, thus enabling new biological functions(2–4). However, in many cases, the functional difference of isozymes is not very well understood. Even for the well-studied single-cell model organism, the baker's yeast *Saccharomyces cerevisiae*, there are many isozymes with unknown functional differences. Here we describe the finding that Target of rapamycin complex 1 (TORC1) differentially regulates the expression of isozymes in yeast and that such regulation helps yeast cells to deal with nutritional stress based on isozymes' distinct enzymatic properties.

hl379@cornell.edu.

Author Contribution: Y. Z. and H.L. designed the experiments and wrote the manuscript. Y. Z. and Z. L. generated yeast strains used in this study. Y. Z. performed SILAC analysis and enzymological studies. Y. Z. and M. W. performed RT-PCR analysis of TDH genes and western blots for ENO and TDH genes.

Supporting Information: Figure S1, biochemical validation of the enolase and GAPDH isozyme expression level changes caused by rapamycin treatment, Figure S2, ALD6 strongly prefers $NADP^+$ as substrate, Table S1, K_m and k_{cat} for ENO1 and ENO2, Table S2, yeast strain used, Table S3, plasmid used, Table S4, list of primers used, Table S5 and Table S6, proteins repressed and induced by chronic rapamycin treatment. This material is available free of charge via the internet at http://pubs.acs.org.

Target of rapamycin (TOR) in yeast functions through one of two large protein complexes, TORC1 and TORC2. TORC2 is rapamycin insensitive and does not respond to nutrient level (5). TORC1 in *saccharomyces cerevisiae* regulates cell growth in response to nutrient availability, energy status, and cellular stress. The inhibition of TORC1 by rapamycin represses general translation, downregulates the production of ribosomes and turns on starvation-specific genes (6–11). Since the discovery of TORC1 in yeast, significant efforts have been taken to identify how cells cope with different stress through TORC1 regulation by proteomics and microarray methods. Most studies examined the effect of TORC1 inhibition on translation with short-term (less than 4 hours) rapamycin treatment (10–14), while chronic consequences remain less well understood. We decided to examine the longer-term (more than 12 hours) effect of TORC1 inhibition on the proteome.

To identify the proteins regulated by TORC1 complex, we performed proteomics studies in *S. cerevisiae* using stable isotope labelling by amino acid in cell culture (SILAC). We cultured BY4741 strain without rapamycin in heavy media and BY4741 with 10 nM rapamycin in light media. After overnight incubation at 30°C, we collected yeast cell at OD600 of 0.5 for both conditions. After lysis, the two samples were mixed, digested with trypsin, and analyzed by mass spectrometry. Proteins with high heavy to light (H/L) ratio are suppressed by rapamycin treatment and proteins with low H/L ratio are induced by rapamycin treatment. Among the list, all the ribosomal proteins are suppressed by rapamycin treatment (Table S5). This is consistent with the known effect of rapamycin and demonstrates that the proteomics data are reliable. Furthermore, we compared the rapamycin regulated proteomics dataset obtained by Bandhakavi and coworkers (15). Among 127 proteins identified in their results, 63 showed similar up or down regulation in our proteomics data.

After analyzing other proteins induced and suppressed by rapamycin, one observation attracted our attention. For a variety of metabolic enzymes, some isoforms are upregulated while others are downregulated (Table 1). The differentially regulated isozymes are present in various metabolic pathways including glycolysis, amino acid biosynthesis, and the pentose phosphate pathway (Table 1).

We next verified the changes in the levels of isozymes identified in the proteomic study. We focused on enzymes in the glycolysis pathway. Using homologous recombination, we tagged several identified isozymes with Flag tag at the endogenous loci on the chromatin. This allowed us to monitor the endogenous protein expression using the Flag tag, overcoming the lack of antibodies for these proteins. After long-term rapamycin treatment, enolase 1 (ENO1) was indeed induced, while enolase 2 (ENO2) was suppressed (Fig S1A). Similarly, for the glyceraldehyde-3-phosphate dehydrogenase (GAPDH) isozymes, we confirmed that TDH1 was induced while TDH3 was suppressed by rapamycin (Fig S1A). We further confirmed that the regulation was transcriptional as the mRNA levels of GAPDH isozymes were changed by rapamycin (Fig S1B). These results convinced us that the proteomic result was reliable.

The above results suggested that although different isozymes share sequence and function similarities, they may have significant differences, which may explain why cells would

express different isozymes under stress conditions. This is similar to the report that cancer cells up-regulates a specific isozyme of pyruvate kinase, PKM2, but not PKM1. PKM2 strongly promotes Warburg effect and cancer cells growth (16). The differentially regulated isozymes may indicate there is a functional difference. The chronic treatment of rapamycin may mimic the growth of yeast with less favored carbon and nitrogen sources. In this condition, yeast needs to upregulate energy production and the biosynthesis of amino acid and nucleotides through gluconeogenesis and pentose phosphate pathways.

Aldehyde dehydrogenase in yeast converts acetaldehyde (from ethanol metabolism) to acetate, producing one molecule of NADH or NADPH (17, 18). Acetate is later used for synthesizing acetyl-CoA for energy production in the TCA cycle (19). ALD2 and ALD3 are well known to be NAD^+-dependent, while ALD4 and ALD6 were annotated as $NADP^+$-dependent. We reasoned that when yeast cells were grown with ethanol as the carbon source, which is not a preferred carbon source, they will need to maximize NADH for energy production by upregulating NAD^+-dependent ALD2 and ALD3 while down regulating $NADP^+$-dependent ALD6. This is consistent with our proteomic data showing increased ALD2/ALD3 and decreased ALD6 with rapamycin treatment. However, the upregulation of ALD4, which is also annotated as an $NADP^+$-dependent enzyme, could not be explained by this.

To investigate this further, we expressed and purified recombinant yeast ALD4 and ALD6 and measured the kinetics of both enzymes. ALD6 can only use $NADP^+$ (Figure S2) but not NAD^+ as its substrate while ALD4 can use both NAD^+ and $NADP^+$ as substrates with similar K_m values (Table 2). As physiological NAD^+ concentration is much higher than $NADP^+$, we reasoned that ALD4 should mainly use NAD^+ as a substrate in physiological conditions. NADH is used in oxidative phosphorylation for energy production while NADPH is used for removing oxidative stress and in several biosynthetic pathways. Under nutrient poor conditions, cells requires NADH for survival and requires less NADPH due to slower cell growth rate and biosynthesis rate. The NADH-generating ALD2, ALD3 and ALD4 may play more important roles than the NADPH-generating ALD6 in nutrient poor conditions. In other words, we predict that deletion of ALD4 would slow down yeast growth more than ALD6 deletion when the cells were grown with ethanol as the sole carbon source. To test this predication, we tested the growth of *ald4Δ* and *ald6Δ* BY4741 strains with ethanol as the carbon source. Indeed, *ald4Δ* showed a more severe growth defect than *ald6Δ* (Fig 1). Furthermore, treatment with 10 mM N-acetyl cysteine (NAC, a reducing reagent), rescued the growth defect of *ald6Δ* but not *ald4Δ*, which is consistent with our enzymology data, suggesting that ALD4 is responsible for NADH production while ALD6 is responsible for NADPH production (Fig 1).

Glycolysis and gluconeogenesis share many enzymes as most of the glycolytic enzymes can catalyze the reverse reactions as well. Based on our hypothesis that under rapamycin treatment, gluconeogenesis should be upregulated, we predicted that the isozymes in glycolysis that are upregulated by rapamycin would favor gluconeogenesis. Enolases catalyze the interconversion between 2-phosphoglycerate (2-PG) and phosphoenolpyruvate (PEP) and play an essential role in glycolysis and gluconeogenesis (20, 21). ENO1 and ENO2 were detected in our proteomic studies with ENO1 upregulated and ENO2

downregulated by rapamycin. To test whether the ENO1 favors gluconeogenesis more than ENO2, we expressed and purified yeast ENO1 and ENO2 from E. *coli* and measured the forward and reverse reaction kinetics of both enzymes with 2-PG and PEP as substrates. As expected, ENO1 showed a higher rate for converting PEP to 2-PG than ENO2 (Table S1 and Fig 2A), while the rates for converting 2-PG to PEP were similar (Table S1 and Fig 2B). The kinetics results indicate that compared to ENO2, ENO1 more favors gluconeogenesis.

To test whether ENO1 promote gluconeogenesis *in vivo*, we monitored yeast growth in media with and without glucose. With glucose as the carbon source, the two strains grew similarly. However, with acetate as the carbon source, *eno1*Δ grew worse than BY4741 (Fig 2D). We further measured glucose concentration in the two strains. The *eno1*Δ strain had lower glucose concentration compared to BY4741 when grown with acetate as the carbon source (Fig 2C). The above data suggest that ENO1 plays a key role in promoting gluconeogenesis when yeasts are grown on acetate.

In summary, in our quantitative proteomics studies to identify proteins that are regulated by chronic rapamycin treatment, we found that for a set of metabolic enzymes, their isoforms are differentially regulated by rapamycin treatment. Further studies indicate that yeast calls on different isoforms of the enzyme under different growth conditions to fit the changing metabolic needs. Under nutrient rich conditions, yeast uses enzymes favoring glycolysis and NADPH production to balance biosynthesis and energy production. Under nutrient poor conditions, which is mimicked by rapamycin treatment, yeast reprograms their metabolic pathways to more efficiently utilize poor carbon source to survive. The observation may well apply to other isozymes identified in this study. As the central hub for nutrient sensing, TORC1 inhibition leads to genome-wide gene expression regulation (7, 22–24). Many of the transcriptional changes, including the metabolic isozyme expression changes, are likely due to the master transcriptional regulator, MSN2/MSN4, which is activated by glucose starvation or rapamycin treatment (22, 23). Although the MSN2/MSN4 DNA binding sequence, CCCCT, is not present in ENO1 and ALD4 promoter sequence, the close-related sequence, such as CCCTT, is present and it is possible that ENO1 and ALD4 are weak target genes of MSN2/MSN4. Alternatively, MSN2/MSN4 may indirectly regulates ENO1 and ALD4. Our study here provides a logical explanation for why different isozymes are turned on under different growth conditions.

The observation that ENO1 favors gluconeogenesis more than ENO2 initially was surprising as it may violate the principle of microscopic reversibility, which predicts that an enzyme should catalyze the forward and reverse reaction equally well. However, the forward and reverse reaction rates are the same only at equilibrium conditions. In cells, enolase almost never works in equilibrium conditions because the glycolysis pathway is a series of chain reactions and the enolase reaction product is quickly converted by the next enzyme. Under such non-equilibrium physiological conditions, it is possible to have enzymes that could favor one of the reaction directions. Similar discussions about enzymes favoring one reaction direction and microscopic reversibility have been reported by other people (25–29).

Isozymes are common in biology. Human cells also contain many isozymes in various metabolic pathways. For example, there are three isocitrate dehydrogenase isozymes as well

as several glutaminase isozymes, which have been implicated in cancer (30–37). Isozymes allow differential regulation of metabolic enzyme to be possible, such as different subcellular localizations and different allosteric regulations. Our studies presented here demonstrate that the intrinsic enzymatic properties of the isozymes (e.g. cofactor choice and forward vs. reverse reaction rates) may also play an important role to enable the different biological functions. It will be of great interest to apply the methods (such as the method to determine the preferred direction of an isozyme) and the concept developed to study the functional differences of isozymes in higher organism including human.

Methods

Yeast Strains.

All strains used in this study are listed in Supplementary Table 2. The strain expressing endogenous FLAG-tagged ENO1, ENO2, TDH1, TDH2 and TDH3 were generated using PCR-based tagging method as previously described(38). Briefly, the PCR fragment amplified from the plasmid pFA6a-6xGLY-3xFLAG-HIS3MX6 (Addgene plasmid 20753) with primers (Table S4) was transformed into BY4741 strain and plated on synthetic complete agar plates with histidine dropout for selection. The *eno1Δ*, single deletion strain was obtained from Open Biosystems (GE Dharmacon).

Sample preparation for SILAC study.

Saccharomyces cerevisiae BY4741 strain (HL813Y) was cultured in synthetic complete media (20 mL) with heavy lysine (Sigma 608041) (0.086 g L^{-1}) and arginine (Sigma 608033) (0.086 g L^{-1}) till OD600 reached approximately 0.5. The BY4741 strain treated with 10 nM Rapamycin was cultured in synthetic complete media with light lysine and arginine till OD600 reached approximately 0.5. Cells were harvested by centrifugation at 5000 rpm for 5 min and lysed with 600 μL of glass beads (OPS Diagnostics BAWG400-200-04) and 1mL lysis buffer containing 50 mM Tris pH 8.0, 150 mM sodium chloride and 1 mM phenylmethanesulfonyl fluoride. Cells were lysed by 5 intervals of vortexing for 1 minutes with 2 minutes cooling on ice between intervals. Total cell lysates were cleared by centrifuging at 17,000 g and 4 °C for 15 min. For each sample, 20 μg of protein from the supernatant was reduced by DTT (10 mM) for 1 hr at RT and alkylated by iodoacetamide (40 mM) for 1 hr at room temperature. The heavy and light samples were then mixed and digested with 1 μg trypsin for 16 hr at 37 °C. The digested peptide mixture was desalted with Waters Sep-Pac® vac C18 1cc column and lipolyzed for 4 hr.

Nano LC/MS/MS and data Analysis of SILAC sample.

The SILAC tryptic digests were reconstituted in 50 μL of 0.5% formic acid (FA) estimated at 0.1 μg μL^{-1} for nanoLC-ESI-MS/MS analysis, which was carried out on an Orbitrap Elite mass spectrometer (Thermo-Fisher Scientific, San Jose, CA) equipped with a “CorConneX” nano ion source device (CorSolutions LLC, Ithaca, NY). The Orbitrap was interfaced with a Dionex UltiMate3000RSLCnano system (Thermo, Sunnyvale, CA). Each SILAC peptide sample (5 μL) was injected under “User Defined Program” onto a PepMap C18 trap column-nano Viper (5 μm, 100 μm × 2 cm, Thermo) at 20 μL min^{-1} flow rate and then separated on a PepMap C18 RP nano column (3 μm, 75 μm × 25 cm, Thermo) which was installed in the

nano device with a 10-μm spray emitter (NewObjective, Woburn, MA). The peptides were eluted with a 120-minute gradient of 5% to 38% acetonitrile (ACN) in 0.1% formic acid at a flow rate of 300 nL min^{-1}, followed by a 7-min ramping to 95% ACN-0.1% FA and a 8-min hold at 95% ACN-0.1% FA. The column was re-equilibrated with 2% ACN-0.1% FA for 25 minutes prior to the next run. The Orbitrap Elite was operated in positive ion mode with nano spray voltage set at 1.6 kV and source temperature at 250 °C with external calibration for FT mass analyzer being performed. The instrument was operated in parallel data-dependent acquisition (DDA) under FT-IT mode using FT mass analyzer for one MS survey scan from m/z 375 to 1800 with a resolving power of 120,000 (FWHM at m/z 400) followed by MS/MS scans on top 20 most intensive peaks with multiple charged ions above a threshold ion count of 10,000 in FT mass analyzer. Dynamic exclusion parameters were set at repeat count 1 with a 30 s repeat duration, an exclusion list size of 500, 60s exclusion duration with ±10 ppm exclusion mass width. Collision induced dissociation (CID) parameters were set at the following values: isolation width 2.0 m/z, normalized collision energy at 35 %, activation Q at 0.25, and activation time 10 ms. All data are acquired under Xcalibur 2.2 operation software (Thermo). All MS and MS/MS raw spectra were processed and searched using Sequest HT software within the Proteome Discoverer 1.4.1.14 (PD 1.4, Thermo Scientific). The Saccharomyces cerevisiae RefSeq sequence database (5,847 entries, downloaded on 5/17/2015 from NCBI nr) was used for database searches. The database search was performed under a search workflow with the “Precursor Ions Quantifier” node for SILAC 2plex (Arg10, Lys8) quantitation. The default setting for protein identification in Sequest node were: two mis-cleavages for full trypsin with fixed carbamidomethyl modification of cysteine, variable modifications of 10.008 Da on Arginine and 8.014 Da on lysine, N-terminal acetylation, methionine oxidation and deamidation of asparagine and glutamine residues. The peptide mass tolerance and fragment mass tolerance values were 15 ppm and 0.8 Da, respectively. Only high confidence peptides defined by Sequest HT with a 1% FDR by Percolator were considered for the peptide identification. The mass precision for expected standard deviation of the detected mass used to create extracted ion chromatograms was set to 3 ppm. The SILAC 2-plex quantification method within PD 1.4 was used with unique peptides only to calculate the heavy/light ratios of all identified proteins without normalization. The final protein group list was further filtered with two peptides per protein in which only #1-rank peptides within top scored proteins were used.

Western Blots.

Yeast grown in 5 mL synthetic complete media with or without rapamycin treatment were collected when OD600 reached 0.5. Yeast pellet was lysed with 200 μL of glass beads in 200 μL buffer containing 25 mM Tris at pH=8.0 and 150 mM NaCl. 1 μg of total yeast lysate was used for western blot against HRP-conjugated anti-Flag antibody (Sigma A8592).

RT-PCR for TDH1, TDH2 and TDH3.

Yeast mRNA was extracted with Qiagene RNeasy Mini Kit following the fourth edition of RNeasy® Mini Handbook with enzymatic lysing with zymolase. The extracted mRNA was reverse transcribed using Invitrogen SuperScript® VILO™ kit. RT-PCR was set up in 384 well plate with technical triplicates in Quantstudio 7 Flex. For each PCR reaction, the reaction system contrains 7.5 μL Sybr green supermixture, 1.5 μL 5 μM foward primer

(Table S4), 1.5 μL 5 μM reverse primer (Table S4), 1 μL cDNA sample (concentration 196.1 ng μL^{-1}) and 3.5 μL water.

Cloning, expression and purification of ALD4 and ALD6.

Genomic DNA was extracted from *Saccharomyces cerevisiae* BY4741 strain using Pierce Yeast DNA Extraction Kit. The DNA sequence encoding for ALD4 with first 23 amino acid truncation and ALD6 was amplified by PCR with primers (Table S4) from the genomic DNA. The amplified gene fragment was inserted into the pET28a vector and transformed into the *Escherichia coli* expression strain BL21 pRARE2. The N-terminal tag from pET28a vector was retained. A single colony was used to inoculate an overnight starter culture, which was used to inoculate 2 liters of LB broth containing 50 μg mL^{-1} kanamycin and 25 μg mL^{-1} chloramphenicol. Cells were grown at 37°C to OD600 of approximately 0.6 and cooled to 16°C. Expression was induced with 1.5 mM isopropyl β-D-1-thiogalactopyranoside (IPTG) and grown overnight at 16°C. Cells were harvested by centrifugation and lysed using the EmulsiFlex-C3 cell disruptor (Avestin, Inc., Canada).

Kinetics measurement of ALD4 and ALD6

For ALD6 kinetics measurement varying concentration of acetaldehyde, 200, 500, 600, 750, 1000, 2000 μM acetaldehyde was incubated in 120 μL of buffer containing 25 mM Tris (pH=7.4), 150 mM NaCl, 1 mM $MgCl_2$ and 1 mM $NADP^+$ at 30 °C in a Cary 50 Bio UV-vis spectrometer (Varian). The production of NADPH at 340 nm was measured. ALD6 was added into the cuvette to final concentration of 1 μM. The slope rate of absorption change was measured. Kinetics data was later fit into Michaelis-Menten equation with GraphPad Prism 5. Kinetics parameters were measured similarly with different concentrations of $NADP^+$ as 50, 100, 250, 375, 500, 1000 μM while maintaining acetaldehyde concentration at 1 mM in the same buffer. ALD4 kinetics measurement was performed similarly by adding acetaldehyde to final concentration at 25, 50, 100, 250, 500, 1000 μM of acetaldehyde in 120 μL of buffer containing 25 mM Tris (pH=7.4), 150 mM NaCl, 1 mM KCl, 1 mM DTT and 1 mM NAD^+. Kinetics parameters for ALD4 in terms of NAD^+ and $NADP^+$ was measured similarly at the NAD^+ or $NADP^+$ concentration of 25, 50, 100, 250, 500, 1000, 2000 μM respectively in 120 μL of buffer containing 25 mM Tris (pH=7.4), 150 mM NaCl, 1 mM KCl, 1 mM DTT and 1 mM acetaldehyde.

Cloning, expression and purification of ENO1 and ENO2.

Genomic DNA was extracted from *Saccharomyces cerevisiae* BY4741 strain using Pierce Yeast DNA Extraction Kit. The DNA sequence encoding for ENO1 and ENO2 was amplified by PCR with primers (Table S4) from the genomic DNA. The amplified gene fragment was inserted into the pET28a vector and transformed into the *Escherichia coli* expression strain BL21 pRARE2. The N-terminal tag from pET28a vector was retained. A single colony was used to inoculate an overnight starter culture, which was used to inoculate 2 liters of LB broth containing 50 μg mL^{-1} kanamycin and 25 μg mL^{-1} chloramphenicol. Cells were grown at 37°C to OD600 of approximately 0.6 and cooled to 16°C. Expression was induced with 1.5 mM isopropyl β-D-1-thiogalactopyranoside (IPTG) and grown overnight at 16°C. Cells were harvested by centrifugation and lysed using the EmulsiFlex-C3 cell disruptor (Avestin, Inc., Canada).

Kinetics measurement of ENO1 and ENO2

10, 20, 50, 100, 200, 500 μM phosphoenolpyruvate or 2-phosphoglycerate was incubated in 120 μL of buffer containing 25 mM Tris and 150 mM NaCl at 30 °C in a Cary 50 Bio UV-vis spectrometer (Varian). The absorption of phosphoenolpyruvate at 240 nm was measured. ENO1 or ENO2 was added into the cuvette to final concentration of 10 nM. The slope rate of absorption change was measured. Kinetics data was later fit into Michaelis-Menten equation using GraphPad Prism 5.

Growth assays for different carbon sources.

Yeast cells were cultured in synthetic complete media at 30°C overnight, dilute to OD600 of 0.2 with synthetic complete media, and then cultured for another 6 hr at 30°C. The OD600 of the culture was dilute to 0.2 with autoclaved water, and then diluted serially in 4-fold increments. Aliquots of each dilution were spotted using a replica plater on synthetic complete agar plates with 2% glucose, 2% potassium acetate or 2% ethanol as carbon source. Plates were incubated at 30°C. Cell growth was recorded 2–3 days after plating.

Glucose concentration measurement.

Yeast BY4741 and *eno1Δ* strains were culture in synthetic media with 2% glucose as carbon source overnight. Both strains were inoculated into synthetic media with 2% potassium acetate as carbon source until OD600 reached 0.5. 10 mL of both strains were collected. Glucose assay kit (abcam65333) was used for measurement. The measurement of glucose concentration follows the protocol provided by abcam65333 protocol booklet.

Supplementary Material

Refer to Web version on PubMed Central for supplementary material.

Acknowledgments:

This work was supported by in part by a grant from the National Institute of Health National Institute of General Medical Sciences (GM 088276). We thank Zhang, S. and Motorykin, I. at the Proteomic and MS Facility of Cornell University for help with the SILAC experiments. The Orbitrap Fusion mass spectrometer is supported by NIH SIG 1S10 OD017992-01 grant. pFA6a-6xGLY-3xFLAG-HIS3MX6 was a gift from Mark Hochstrasser (Addgene plasmid # 20753).

References

1. Markert CL, and Møller F (1959) MULTIPLE FORMS OF ENZYMES: TISSUE, ONTOGENETIC, AND SPECIES SPECIFIC PATTERNS, Proc. Natl. Acad. Sci. U. S. A 45, 753–763. [PubMed: 16590440]
2. Henderson NS (1965) Isozymes of Isocitrate Dehydrogenase: Subunit Structure and Intracellular Location, J. Exp. Zool 158, 263–273. [PubMed: 14327193]
3. Pearce JM, Edwards YH, and Harris H (1976) Human enolase isozymes: electrophoretic and biochemical evidence for three loci, Ann. Hum. Genet 39, 263–276. [PubMed: 5939]
4. Jornvall H, Fairwell T, Kratofil P, and Wills C (1980) Differences in alpha-amino acetylation of isozymes of yeast alcohol dehydrogenase, FEBS Lett 111, 214–218. [PubMed: 6987085]
5. Loewith R, Jacinto E, Wullschleger S, Lorberg A, Crespo JL, Bonenfant D, Oppliger W, Jenoe P, and Hall MN (2002) Two TOR complexes, only one of which is rapamycin sensitive, have distinct roles in cell growth control, Mol. Cell 10, 457–468. [PubMed: 12408816]

6. Barbet NC, Schneider U, Helliwell SB, Stansfield I, Tuite MF, and Hall MN (1996) TOR controls translation initiation and early G1 progression in yeast, Mol. Biol. Cell 7, 25–42. [PubMed: 8741837]
7. Beck T, and Hall MN (1999) The TOR signalling pathway controls nuclear localization of nutrient-regulated transcription factors, Nature 402, 689–692. [PubMed: 10604478]
8. Cardenas ME, Cutler NS, Lorenz MC, Di Como CJ, and Heitman J (1999) The TOR signaling cascade regulates gene expression in response to nutrients, Genes Dev 13, 3271–3279. [PubMed: 10617575]
9. Heitman J, Movva NR, and Hall MN (1991) Targets for cell cycle arrest by the immunosuppressant rapamycin in yeast, Science 253, 905–909. [PubMed: 1715094]
10. Jefferies HB, Fumagalli S, Dennis PB, Reinhard C, Pearson RB, and Thomas G (1997) Rapamycin suppresses 5'TOP mRNA translation through inhibition of p70s6k, EMBO J 16, 3693–3704. [PubMed: 9218810]
11. Martin DE, Soulard A, and Hall MN (2004) TOR regulates ribosomal protein gene expression via PKA and the Forkhead transcription factor FHL1, Cell 119, 969–979. [PubMed: 15620355]
12. Thoreen CC, Chantranupong L, Keys HR, Wang T, Gray NS, and Sabatini DM (2012) A unifying model for mTORC1-mediated regulation of mRNA translation, Nature 485, 109–113. [PubMed: 22552098]
13. Huang J, Zhu H, Haggarty SJ, Spring DR, Hwang H, Jin F, Snyder M, and Schreiber SL (2004) Finding new components of the target of rapamycin (TOR) signaling network through chemical genetics and proteome chips, Proc. Natl. Acad. Sci. U. S. A 101, 16594–16599. [PubMed: 15539461]
14. Grolleau A, Bowman J, Pradet-Balade B, Puravs E, Hanash S, Garcia-Sanz JA, and Beretta L (2002) Global and specific translational control by rapamycin in T cells uncovered by microarrays and proteomics, J. Biol. Chem 277, 22175–22184. [PubMed: 11943782]
15. Bandhakavi S, Xie H, O'Callaghan B, Sakurai H, Kim D-H, and Griffin TJ (2008) Hsf1 Activation Inhibits Rapamycin Resistance and TOR Signaling in Yeast Revealed by Combined Proteomic and Genetic Analysis, PLOS ONE 3, e1598. [PubMed: 18270585]
16. Christofk HR, Vander Heiden MG, Harris MH, Ramanathan A, Gerszten RE, Wei R, Fleming MD, Schreiber SL, and Cantley LC (2008) The M2 splice isoform of pyruvate kinase is important for cancer metabolism and tumour growth, Nature 452, 230. [PubMed: 18337823]
17. Meaden PG, Dickinson FM, Mifsud A, Tessier W, Westwater J, Bussey H, and Midgley M (1997) The ALD6 gene of Saccharomyces cerevisiae encodes a cytosolic, Mg(2+)-activated acetaldehyde dehydrogenase, Yeast 13, 1319–1327. [PubMed: 9392076]
18. Tessier WD, Meaden PG, Dickinson FM, and Midgley M (1998) Identification and disruption of the gene encoding the K(+)-activated acetaldehyde dehydrogenase of Saccharomyces cerevisiae, FEMS Microbiol. Lett 164, 29–34. [PubMed: 9675847]
19. Boubekeur S, Bunoust O, Camougrand N, Castroviejo M, Rigoulet M, and Guerin B (1999) A mitochondrial pyruvate dehydrogenase bypass in the yeast Saccharomyces cerevisiae, J. Biol. Chem 274, 21044–21048. [PubMed: 10409655]
20. Entian KD, Meurer B, Kohler H, Mann KH, and Mecke D (1987) Studies on the regulation of enolases and compartmentation of cytosolic enzymes in Saccharomyces cerevisiae, Biochim. Biophys. Acta 923, 214–221. [PubMed: 3545298]
21. McAlister L, and Holland MJ (1982) Targeted deletion of a yeast enolase structural gene. Identification and isolation of yeast enolase isozymes, J. Biol. Chem 257, 7181–7188. [PubMed: 6282834]
22. De Wever V, Reiter W, Ballarini A, Ammerer G, and Brocard C (2005) A dual role for PP1 in shaping the Msn2-dependent transcriptional response to glucose starvation, EMBO J 24, 4115–4123. [PubMed: 16281053]
23. Gorner W, Durchschlag E, Wolf J, Brown EL, Ammerer G, Ruis H, and Schuller C (2002) Acute glucose starvation activates the nuclear localization signal of a stress-specific yeast transcription factor, EMBO J 21, 135–144. [PubMed: 11782433]

24. Schmitt AP, and McEntee K (1996) Msn2p, a zinc finger DNA-binding protein, is the transcriptional activator of the multistress response in Saccharomyces cerevisiae, Proc. Natl. Acad. Sci. U. S. A 93, 5777–5782. [PubMed: 8650168]
25. Krupka RM, Kaplan H, and Laidler KJ (1966) Kinetic consequences of the principle of microscopic reversibility, Trans. Faraday. Soc 62, 2754–2759.
26. Alberty RA (1953) The Effect of Enzyme Concentration on the Apparent Equilibrium Constant for an Enzyme-catalyzed Reaction, J. Am. Chem. Soc 75, 1925–1928.
27. Uhr ML (1979) The Influence of an enzyme on the direction of a reaction, Biochem. Edu 7, 15–17.
28. Krieg AF, Rosenblum LJ, and Henry JB (1967) Lactate dehydrogenase isoenzymes a comparison of pyruvate-to-lactate and lactate-to-pyruvate assays, Clin. Chem 13, 196–203. [PubMed: 6018717]
29. Ross JM, Oberg J, Brene S, Coppotelli G, Terzioglu M, Pernold K, Goiny M, Sitnikov R, Kehr J, Trifunovic A, Larsson NG, Hoffer BJ, and Olson L (2010) High brain lactate is a hallmark of aging and caused by a shift in the lactate dehydrogenase A/B ratio, Proc. Natl. Acad. Sci. U. S. A 107, 20087–20092. [PubMed: 21041631]
30. Reitman ZJ, and Yan H (2010) Isocitrate Dehydrogenase 1 and 2 Mutations in Cancer: Alterations at a Crossroads of Cellular Metabolism, J. Natl. Cancer. Inst 102, 932–941. [PubMed: 20513808]
31. Dang L, White DW, Gross S, Bennett BD, Bittinger MA, Driggers EM, Fantin VR, Jang HG, Jin S, Keenan MC, Marks KM, Prins RM, Ward PS, Yen KE, Liau LM, Rabinowitz JD, Cantley LC, Thompson CB, Vander Heiden MG, and Su SM (2009) Cancer-associated IDH1 mutations produce 2-hydroxyglutarate, Nature 462, 739–744. [PubMed: 19935646]
32. Jiang L, Shestov AA, Swain P, Yang C, Parker SJ, Wang QA, Terada LS, Adams ND, McCabe MT, Pietrak B, Schmidt S, Metallo CM, Dranka BP, Schwartz B, and DeBerardinis RJ (2016) Reductive carboxylation supports redox homeostasis during anchorage-independent growth, Nature 532, 255–258. [PubMed: 27049945]
33. Cassago A, Ferreira AP, Ferreira IM, Fornezari C, Gomes ER, Greene KS, Pereira HM, Garratt RC, Dias SM, and Ambrosio AL (2012) Mitochondrial localization and structure-based phosphate activation mechanism of Glutaminase C with implications for cancer metabolism, Proc. Natl. Acad. Sci. U. S. A 109, 1092–1097. [PubMed: 22228304]
34. Hu W, Zhang C, Wu R, Sun Y, Levine A, and Feng Z (2010) Glutaminase 2, a novel p53 target gene regulating energy metabolism and antioxidant function, Proc. Natl. Acad. Sci. U. S. A 107, 7455–7460. [PubMed: 20378837]
35. Erickson JW, and Cerione RA (2010) Glutaminase: A Hot Spot For Regulation Of Cancer Cell Metabolism?, Oncotarget 1, 734–740. [PubMed: 21234284]
36. Mates JM, Campos-Sandoval JA, and Marquez J (2018) Glutaminase isoenzymes in the metabolic therapy of cancer, Biochim. Biophys. Acta 24, 007.
37. Mates JM, Segura JA, Martin-Rufian M, Campos-Sandoval JA, Alonso FJ, and Marquez J (2013) Glutaminase isoenzymes as key regulators in metabolic and oxidative stress against cancer, Curr. Mol. Med 13, 514–534. [PubMed: 22934847]
38. Funakoshi M, and Hochstrasser M (2009) Small epitope-linker modules for PCR-based C-terminal tagging in Saccharomyces cerevisiae, Yeast 26, 185–192. [PubMed: 19243080]

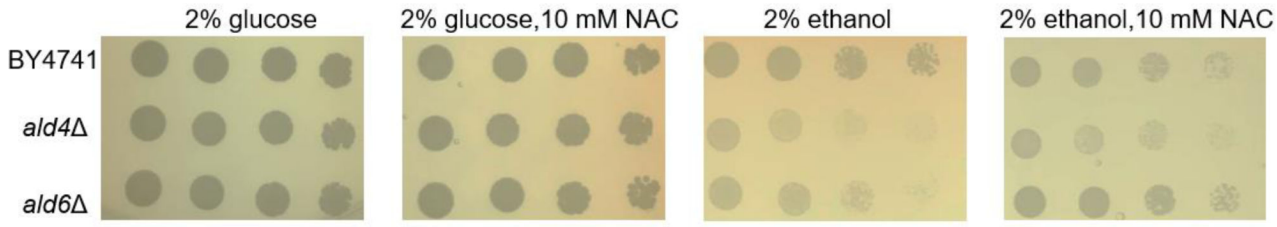

Figure 1.

ALD4 promotes yeast cell growth on ethanol as the carbon source. Growth of BY4741, *ald4Δ* and *ald6Δ* on ethanol or glucose as carbon source with or without N-acetyl cysteine as indicated. The strains used are specified on the left. Each row represents a serial dilution from left to right.

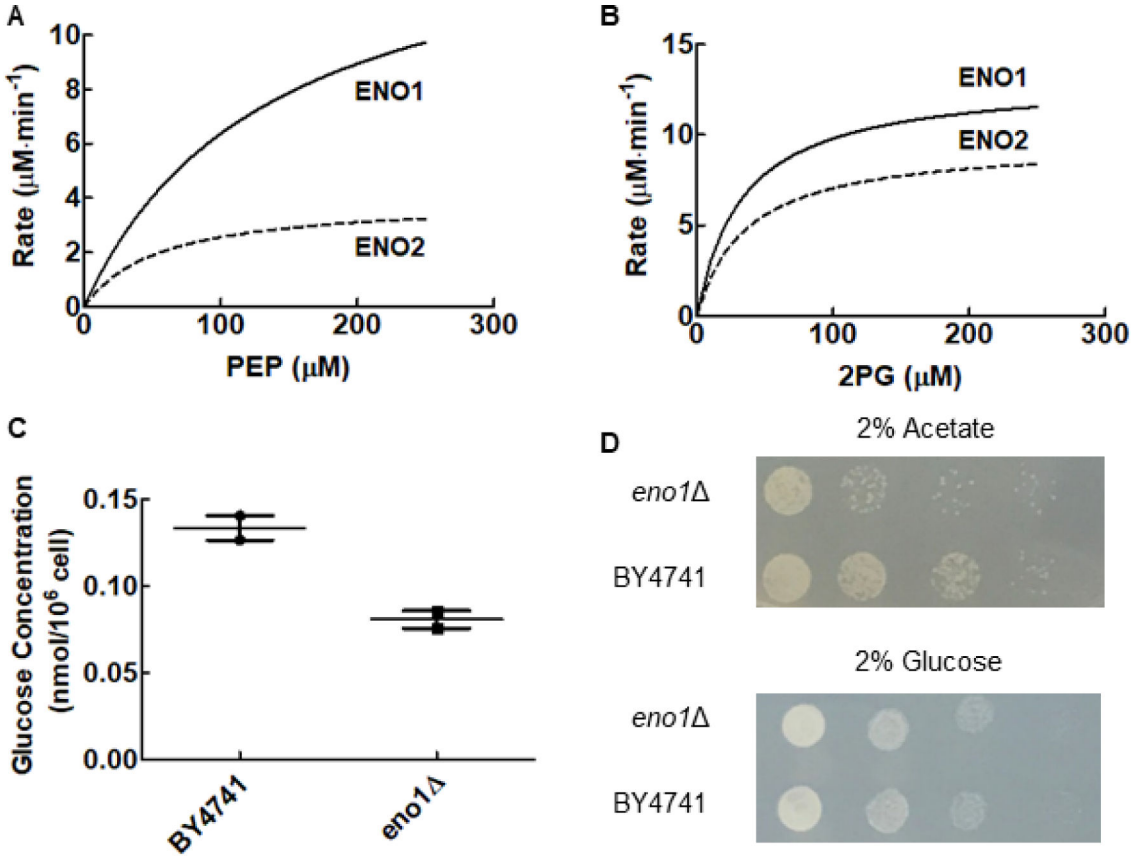

Figure 2.

ENO1 promotes gluconeogenesis in yeast. (A, B) Michaelis-Menten plots for ENO1 and ENO2 with phosphoenolpyruvate (A) or 2-phosphoglycerate (B) as substrate. (C) The glucose concentration of BY4741 and *eno1Δ* grown in synthetic media with acetate as carbon source. (D) Growth of BY4741 and *eno1Δ* on acetate or glucose as carbon source. The strains used are specified on the left. Each row represents a serial dilution from left to right.

Table 1.

Isozymes regulated differently with rapamycin treatment

Pathway	Protein	Regulation by rapamycin
Amino Acid Biosynthesis	2-isopropylmalate synthase LEU4	up
	2-isopropylmalate synthase LEU9	down
	asparagine synthase (glutamine-hydrolyzing) ASN1	up
	asparagine synthase (glutamine-hydrolyzing) ASN2	down
Glycolysis	glyceraldehyde-3-phosphate dehydrogenase (phosphorylating) TDH1	up
	glyceraldehyde-3-phosphate dehydrogenase (phosphorylating) TDH2	down
	glyceraldehyde-3-phosphate dehydrogenase (phosphorylating) TDH3	down
	phosphoglucomutase PGM1	down
	phosphoglucomutase PGM2	up
	phosphopyruvate hydratase ENO1	up
	phosphopyruvate hydratase ENO2	down
	aldehyde dehydrogenase (NAD^+) ALD2	up
	aldehyde dehydrogenase (NAD^+) ALD3	up
	aldehyde dehydrogenase ($NADP^+$) ALD4	up
	aldehyde dehydrogenase ($NADP^+$) ALD6	down
Pentose phosphate pathway	phosphogluconate dehydrogenase (decarboxylating) GND1	down
	phosphogluconate dehydrogenase (decarboxylating) GND2	up
	transketolase TKL1	down
	transketolase TKL2	up

Table 2.

K_m and k_{cat} values for ALD4 and ALD6

Enzyme	Substrate	K_m (μM)	k_{cat} (min^{-1})
	Acetaldehyde	210 ± 40	24 ± 2
ALD4	NAD^+	530 ± 40	29.6 ± 0.8
	$NADP^+$	500 ± 60	13.6 ± 0.6
	Acetaldehyde	600 ± 100	40 ± 4
ALD6	NAD^+	ND	ND
	$NADP^+$	280 ± 40	33 ± 2

ND: not detectable.